First International Symposium on Mine Safety Science and Engineering

The numerical simulation on the regularity of dust dispersion in whole-rock mechanized excavation face with different air-draft amount

NIE Wen, CHENG Wei-min, ZHOU Gang, YAO Yu

[a]Key laboratories of coal mine disaster prevention and control, College of Resources and Environmental Engineering, Shandong university of science and technology, Qingdao 266510, China;

Abstract

The k-ε equation and the k-ε-Θ-k_p equation established with eulerian-eulerian method and eulerian-lagrangian method were used to build the mathematical model of solving single-phase air flow in whole-rock mechanized excavation face and two-phase flow of gas and dust particles. Moreover, based on collocated grid SIMPLE algorithm, using FLUENT software, this paper simulated the pressure distribution of air-flowing field in whole-rock mechanized excavation face with different air-draft amount and dust dispersion. The result shows that the differential pressure value is becoming bigger and bigger between extraction fan drum and ambient environment, de-dust ability of extraction fan drum is gathering strength, pervasion intensity of producing dust is continuously decreased in tunneling place, the mean dust concentration of driver position and whole section was decreased 51.28% and 56.51% respectively, and diffusion distance of high dust concentration has reduced from 13.6m to 8.5m, when the air draft volume changed from 320m^3/min to 600m^3/min. Comparing with measuring results of the experiment, the dust concentration of simulation value and the fact value are basically identical in measuring points work face. All these suggest that the simulation results have good reflection.

Selection and/or peer-review under responsibility of China Academy of Safety Science and Technology, China University of Mining and Technology(Beijing), McGill University and University of Wollongong.

* Corresponding author. Tel.: +86 13793296187; fax: +86 0532-86057013.
E-mail address: sdniewen@163.com.

1. Introduction

In recent years, in order to improve the efficiency of the whole-rock roadway excavation, partial mines of high yield and high efficiency in our country have gradually developed whole-rock tunnel coal drift technology in place of the traditional digging and blasting technology, greatly raising its excavation speed. However, with the improvement of mechanization degree, its dust producing amount have increased dramatically. What's worse is that higher SiO_2 content in rock dust results in a serious threat to underground workers' health (ZHAO Yongnian 2011) [1-3]. At present, each of major coal-producing kingdoms in the word in the aspect of coal mining mechanized excavation face has widely applied forced-exhaust ventilation that has worked well in dust removal with drawing-type partial blower for dusting fan. Since toxic and harmful gas in the whole-rock heading face is less, The amount of exhaust ventilation in general ventilation mode larger than the press-ventilation should be adopted to improve dust removal effect, ironically, due to the more capriciousness in choosing suitable air-draft amount, the optimal air-draft amount appropriate for the whole-rock roadway driving working face cannot be picked out (CHENG Weimin 2009) [4-6]. The crux of the problems above lies in the insufficient understanding of the regularity of dust dispersion in whole-rock mechanized excavation face with different air-draft amount. Furthermore, the flow law of gas-dust flow field is a complex flow process in the extreme, with many factors, and also hard to be obtained directly by model tests and field measurement. Therefore, numerical simulation becomes very important for studies on the flow field (WANG Xiaozhen 2007) [7]. In order to solve the above problem, Ansys Fluent12.1 fluid simulation software is adopted to choose the optimal air-draft amount by simulating the regularity of dust dispersion in whole-rock mechanized driving working face with different air-draft amount.

2. The mathematical model and numerical solution

Use the double k-ε equation model by eulerian method and establish mathematical model of single-phase air flow in the whole-rock mechanized excavation face (ZHANG Jing 2008) [9-11]. Based on the model, aiming at characteristics of two-phase flow of gas and dust particles, apply eulerian-eulerian method and eulerian-lagrangian method and establish k-ε-Θ-k_p mathematical model to solve the regularity of dust dispersion in space. Therefore particle phase stress can be derived, such as the expression of the particle phase viscosity and pressure and closed equations suitable for describing particle flow (ZHOU Lixing 2003) [10, 12, 13].The two-phase flow of gas and dust particles in the whole-rock mechanized excavation face is normally in turbulent state. Therefore, k-ε-Θ-k_p model include the Reynolds time-averaged turbulence model equations of particle phase and gas phase.

Two phase control equations of Turbulent gas phase and turbulent particle phase can be as follows:

Continuity equation of gas phase:

$$\frac{\partial (\alpha\rho)_q}{\partial t} + \frac{\partial (\alpha\rho\vec{U}_i)_q}{\partial x_i} = -\frac{\partial}{\partial x_i}\left[\overline{(\alpha\rho)_q^{'}\vec{U}_{i,q}^{'}}\right] \tag{1}$$

Among them, q for gas phase; α for control body volume fraction of gas phase; $\vec{U}$ for velocity vector, m/s; t for time vector, s; i for an index sign of tensor, i= 1, 2, 3.

Continuous equation of particle density:

$$\frac{\partial (\alpha\rho)_p}{\partial t} + \frac{\partial (\alpha\rho\vec{U}_i)_p}{\partial x_i} = -\frac{\partial}{\partial x_i}\left(\overline{(\alpha_p\rho_p)^{'}\vec{U}_{i,p}^{'}}\right) \tag{2}$$

Momentum equations of gas phase:

$$\frac{\partial\left(\alpha\rho\vec{U}_j\right)_q}{\partial t}+\frac{\partial\left(\alpha\rho\vec{U}_i\vec{U}_j\right)_q}{\partial x_i}=-\alpha_q\frac{\partial P}{\partial x_j}+\alpha_q\rho_q g_j+\frac{\partial\tau_{i,j}}{\partial x_i}+\beta_j\left(\vec{U}_{j,p}-\vec{U}_{j,q}\right)-\frac{\partial}{\partial x_i}\left(\alpha_q\rho_q\overline{\vec{U}'_{i,q}\vec{U}'_{j,p}}\right) \quad (3)$$

$$\tau_{i,j}=\mu_q\left[\left(\frac{\partial\vec{U}_{j,q}}{\partial x_i}+\frac{\partial\vec{U}_{i,q}}{\partial x_j}\right)-\frac{2}{3}\delta_{i,j}\frac{\partial\vec{U}_{k,q}}{\partial x_k}\right] \quad (4)$$

Momentum equations of particles (Martin Sommerfeld, 2001) [11-12]:

$$\frac{\partial\left(\alpha\rho\vec{U}_j\right)_p}{\partial t}+\frac{\partial\left(\alpha\rho\vec{U}_i\vec{U}_j\right)_p}{\partial x_i}=-\alpha_p\frac{\partial p}{\partial x_j}+\rho_p g_j+\frac{\partial\Pi_{i,j}}{\partial x_i}+\beta_j\left(\vec{U}_{j,q}-\vec{U}_{j,p}\right)-\frac{\partial}{\partial x_i}\left(\alpha_p\rho_p\overline{\vec{U}'_{j,p}\vec{U}'_{i,p}}\right)$$

$$-\frac{\partial}{\partial x_i}\left(\vec{U}_{j,p}\overline{\left(\alpha_p\rho_p\right)'\vec{U}'_{i,p}}+\vec{U}_{i,p}\overline{\left(\alpha_p\rho_p\right)'\vec{U}'_{j,p}}\right) \quad (5)$$

The temperature Θ equation of particles (Soo S. L., 1989) [13]

$$\frac{3}{2}\left[\frac{\partial}{\partial t}\left(\alpha\rho\Theta\right)_p+\frac{\partial}{\partial x_i}\left(\alpha\rho\vec{U}_i\Theta\right)_p\right]=\Pi_{i,j}\frac{\partial\vec{U}_{j,p}}{\partial x_i}+\frac{\partial}{\partial x_i}\left[\Gamma\frac{\partial\Theta}{\partial x_i}\right]-\gamma-\frac{3}{2}\alpha_p\rho_p\overline{\vec{},p}$$

$$-\frac{3}{2}\frac{\partial}{\partial x_i}\left(\Theta\overline{\left(\alpha_p\rho_p\right)\vec{U}'_{i,p}}+\vec{}_{i,p}\overline{\left(\alpha_p\rho_p\right)'}\right) \quad (6)$$

Formula 2 to 6, *p* is particles phase and k is index notation of tensor; β_j is the gas-particle drag coefficient between the components in the *j* direction; *p* is pressure, Pa; γ is the dissipation of collision energy, Γ_Θ is the transport coefficient of particles temperature, ξ_p is the whole viscosity of particles phase; μ_p is the shear viscosity of particles phase.

Equation of gas turbulent energy:

$$\frac{\partial}{\partial t}\left(\alpha_q\rho_q k\right)+\frac{\partial}{\partial x_j}\left(\alpha_q\rho_q\vec{U}_{j,q}k\right)=\frac{\partial}{\partial x_j}\left(\frac{\mu_e}{\sigma_k}\frac{\partial k}{\partial x_j}\right)+G_k+G_p-\alpha_q\rho_q\varepsilon \quad (7)$$

Equation of gas dissipation rate of turbulent energy:

$$\frac{\partial}{\partial t}\left(\alpha_q\rho_q\varepsilon\right)+\frac{\partial}{\partial x_j}\left(\alpha_q\rho_q\vec{U}_{j,q}\varepsilon\right)=\frac{\partial}{\partial x_j}\left(\frac{\mu_e}{\sigma_k}\frac{\partial\varepsilon}{\partial x_j}\right)+\frac{\varepsilon}{k}\left[C_1\left(G_k+G_p\right)-C_2\alpha_q\rho_q\varepsilon\right] \quad (8)$$

Among them,

$$G_k=\mu_{q,t}\left(\frac{\partial\vec{U}_{i,q}}{\partial x_j}+\frac{\partial\vec{U}_{j,q}}{\partial x_i}\right)\frac{\partial\vec{U}_{i,q}}{\partial x_j},\ G_p=\frac{2\alpha_p\rho_p}{\tau_p}\left(C_p^p\sqrt{k\left(k_p+\Theta\right)}-k\right);\ \mu_e=\mu_q+\mu_{q,t};$$

$$\mu_{q,t}=C_\mu\alpha_q\rho_q\frac{k^2}{\varepsilon}.$$

k_p turbulent energy equation of particles (YU Minggao 2009) [14-16]:

$$\frac{\partial}{\partial t}\left(\alpha_p\rho_p k_p\right)+\frac{\partial}{\partial x_k}\left(\alpha_p\rho_p\vec{U}_{p,k}k_p\right)=\frac{\partial}{\partial x_k}\left(\frac{\mu_{p,t}}{\sigma_\varepsilon}\frac{\partial k_p}{\partial x_k}\right)+G_{kp}-\alpha_p\rho_p\varepsilon_p+\frac{\partial}{\partial x_k}\left(k_p\frac{\mu_{p,t}}{\sigma_\varepsilon}\frac{\partial\alpha_p\rho_p}{\partial x_k}\right) \quad (9)$$

Using the above model is closed, three-dimensional cylindrical coordinate system in the steady-state control of turbulent two-phase flow equations can be expressed in general form, namely: convective phase=diffusion + convection source term.

The general expression of equations of control gas phase:

$$\frac{\partial}{\partial x}\left(\alpha_g \rho_g u\varphi\right) + \frac{\partial}{r\partial r}\left(r\alpha_g \rho_g v\varphi\right) + \frac{\partial}{r\partial \theta}\left(\alpha_g \rho_g w\varphi\right) = \frac{\partial}{\partial x}\left(\Gamma_\varphi \frac{\partial \varphi}{\partial x}\right) + \frac{\partial}{r\partial r}\left(r\Gamma_\varphi \frac{\partial \varphi}{\partial r}\right)$$

$$+ \frac{\partial}{r^2\partial \theta}\left(\Gamma_\varphi \frac{\partial \varphi}{\partial \theta}\right) + S_\varphi + S_{\varphi p} \tag{10}$$

The general expression of equations control dust particles:

$$\frac{\partial}{\partial x}\left(\alpha u_p \varphi_p\right) + \frac{\partial}{r\partial r}\left(r\alpha v_p \varphi_p\right) + \frac{\partial}{r\partial \theta}\left(\alpha w_p \varphi_p\right) = \frac{\partial}{\partial x}\left(\Gamma_{\varphi p} \frac{\partial \varphi_p}{\partial x}\right) + \frac{\partial}{r\partial r}\left(r\Gamma_{\varphi p} \frac{\partial \varphi_p}{\partial r}\right)$$

$$+ \frac{\partial}{r^2\partial \theta}\left(\Gamma_{\varphi p} \frac{\partial \varphi_p}{\partial \theta}\right) + S_{\varphi p} + S_{\varphi pg} \tag{11}$$

From formula 8 to 11, turbulence model constants C_1, C_2, C_μ, σk and C_p^p respect 1.44,1.92,0.09,1.0 and 0.85 (Martin Sommerfeld, 2001) [11-16].

When models above are established, first discretize the equations with the help of the finite volume and the use of mixed mesh division, and then figure out the numbers of the dust with the help of the mixed mesh division and the simple arithmetic.

3. Physical models and boundary conditions

3.1. Physical and geometric models and mesh division

With the help of the Gambit software, established the proportional physical and geometric model of the hybrid ventilation system of main return way in Tangkou coal mine and the established model was further mesh divided. The internet size of model mesh was hexahedral and the physical and geometric models before and after the division is illustrated in figure 1:
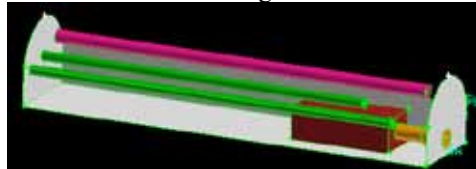
(a) Geometry Model
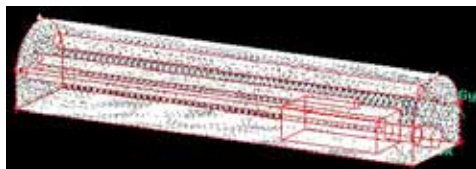
(b) After Meshing

Fig.1. Geometry model and its meshing

The established model consists of four parts: the tunnel, the entry-driving machine, the pressed-type washroom and the drawer-type washroom. The tunnel is a semicircle arch area with the length of 25.0m, the width of 5.44m and the height of 4.68m. The entry-driving machine is 9.0m long and its body is a cuboid with the length of 6.0m, the width of 2.7m and the height of 1.96m. The cutting arm is a cylinder with its length as 1.8m and the diameter as 0.9m; the cutting head is a cylinder 1.2m long and its diameter is 1.2m. The pressed-type washroom is a cylinder about 2m away from the cutting head, its length is 23m and its diameter is 0.8m. The central axis is 3m away from the ground and 0.1m from the nearest tunnel wall. The amount of air pressed is 280m^3/min, the two drawer-type washroom was two cylinders and the one in the middle is 5m away from the cutting head and its length is 20m and its diameter is 0.6m. The central axis is 2.36m from the ground; the one on the side is 2.5m away from the cutting head and its length is 22.5m and the diameter is 0.6m. Its central axis is 1.96m from the ground. In the established model, the *z*-direction is the direction of the length of the tunnel, the *x*-direction is the direction of the width of the tunnel and the *y*-direction is the direction of the height of the tunnel. The positive direction along *z*-axis is the direction from the cutting head to the end of the tunnel, The positive direction along *x*-axis is the direction from one side of the tunnel to the other side of the tunnel, and the positive direction along *y*-axis is the direction from the base board of the tunnel to the ceiling board of the tunnel.

3.2. The boundary condition of the numerical simulation and the parameter for the granule

Table 1. Boundary conditions and the main parameters for the dust source setting

Item	Name	The setting of the parameters
Boundary conditions	the type of the entrance boundary	Velocity-inlet
	the wind speed of the tunnel (*m/s*)	0.38888
	turbulence dynamic energy	0.8
	turbulence diffusion ratio (m^2/s^3)	0.8
	the type of the exit boundary	Outflow
Main parameters for the dust source	the distribution of dust particle diameter	Rosin-rammler
	the sending-out speed of the dust (*kg/s*)	2×10^{-3}
	the minimal grain diameter (*m*)	0.85×10^{-6}
	the maximal grain diameter (*m*)	3.185×10^{-5}
	the distribution parameter	1.77
	the tracking times	3200
	the temperature of the dusts (m^2/s^2)	0.08

In order to study the influence of the amount of the pumping air on the hybrid ventilation dust flow field, made a numerical simulation of the regularity of distribution of the air flow and the regularity of distribution of the air flow in the partial ventilation system under different circumstances (the whole amount of the pumping air is 320m^3/min, the amount of the pumping air in the central part is 163m^3/min and the amount of the pumping air on the side is 157m^3/min) in the coal mine.

4. Simulation results analysis on the regularity of pressure distribution in Air-flowing Field

Show air-flowing pressure field in the whole machined driving working face through the contour map of pressure. Meanwhile, it also analyzes specific simulation figure on the regularity of pressure

distribution in air-flowing field in four sections located in x=2.72m (the position in the direction of axis of drawer type fan drum in the middle of the roadway along the x), x=4.47m (the position in the direction of axis of drawer type fan drum in the lateral part of the roadway along the x), y=1.96m (the section on the height of axis of drawer type fan drum in the lateral part of the roadway), y=2.36m (the section on the height of axis of drawer type fan drum in the middle of the roadway). When the total amount of air draft is 600m³/min the overall pressure distribution in air-flowing field and pressure distribution of the section in axis of drawer type fan drum which are respectively listed in figure 2 , figure 3 and table 2 is different value of pressure between drawer type fan drum and surroundings with different amount of air draft. Among them, A stands for pressure differential value between the tunneling place and surroundings, while B is pressure differential value between the mouth of fan drum and surroundings.
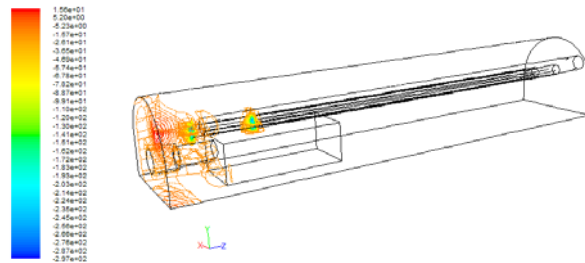
Fig. 2. The total amount of pumping air is 600m³/min, the wind field of pressure distributes in the roadway

(a) x=2.72

(b) x=4.47

(c) y=1.96
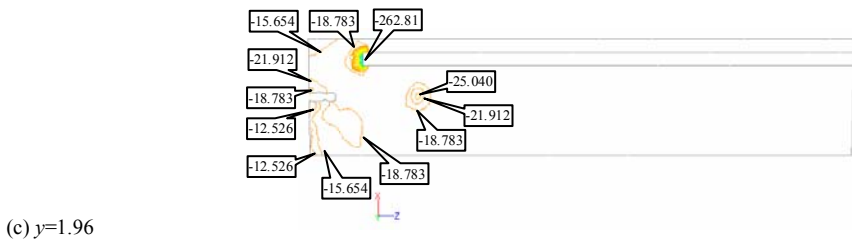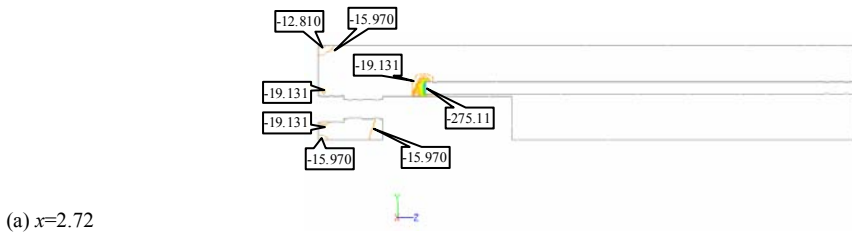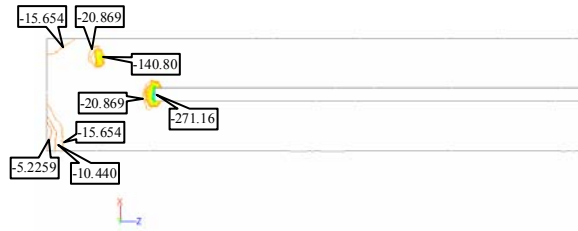
(d) y=2.36

Fig. 3. The drawing-type fan drum pressure distributes of extraction fan drumwhen the amount of pumping air is 600m^3/min in axis section

Table 2. Differential pressure between different drawing fan drums and ambient environment

The amount of pumping air	x=2.72m		y=2.36m		x=4.47m		y=1.96m	
	A (Pa)	B (Pa)	A (Pa)	B (Pa)	A (Pa)	B (Pa)	A (Pa)	B (Pa)
320m^3/min	81.535	77.653	79.687	79.687	60.180	56.298	60.180	56.298
400m^3/min	111.087	106.895	116.9317	100.987	110.663	106.840	103.542	99.821
450m^3/min	148.720	143.929	156.0612	139.340	151.117	146.319	139.127	134.329
500m^3/min	171.913	166.54	177.2807	161.164	171.913	166.540	171.906	168.600
550m^3/min	209.365	203.855	215.435	196.426	208.097	202.761	206.980	202.761
600m^3/min	262.300	255.979	265.9341	250.291	265.934	259.677	250.284	244.027
Pressure difference increase amplitude (Pa)	180.765	178.326	186.2471	170.604	205.754	203.379	190.104	187.729

From the simulation results above, we can get the results:

(1) With the amount of the pumping air, within the field of z=5m~25m, the pressure is within the scope of -18.922Pa~-12.294Pa, which is quite even. From this we can conclude that when the amount of the pumping air is stable, the pressure in the drawer-type washroom will keep stable.

(2)When the amount of the pumping air increases from 320m^3/min to 600m^3/min, the difference of the pressure between the central axis and the cutting head increases, and the difference is within the scope of 170.604Pa~190.104Pa, which suggests that with the increase of the amount of the pumping air, the ability of the drawer-type washroom also increases and such ability peaks when the amount of the pumping air is 600m^3/min.

(3)The pressure difference between the cutting head is greater than the pressure difference on the sides, which suggests that ability of the side part of the drawer-type washroom is greater than the central part, which may be the result of the pressed-type washroom being on one side of the tunnel and thus most of the pressed air flowing from its opposite. What is more, the drawer-type washroom on the side is closer to the cutting head, so it led to be greater pressure differential.

5. The analysis of the simulation of the regularity of the dust distribution

Figure 4 illustrates the variation tendency of the dust distribution at the place of 0m, 1m, 1.55m, 1.96m (the breathing height of workers except driver), 2.36m, 4m along the positive y-direction. In order to study the dust distribution in different pumping air conditions, we analyzed the dust density in the

place of *y*=1.55m and *z*=5.2m, as illustrated in fig.5, C is the diffusion length of the high-density dust when y is 1.55m and D and E are the average dust density when *z*=5.2m.
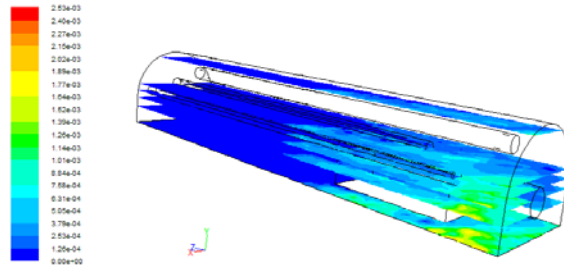
(a) 320m³/min
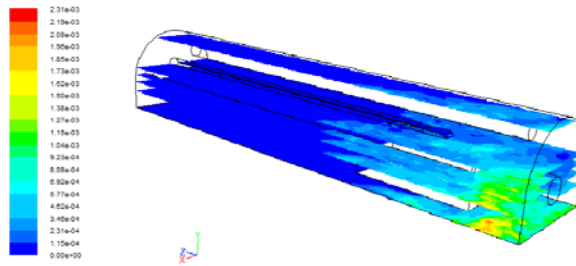
(b) 400m³/min
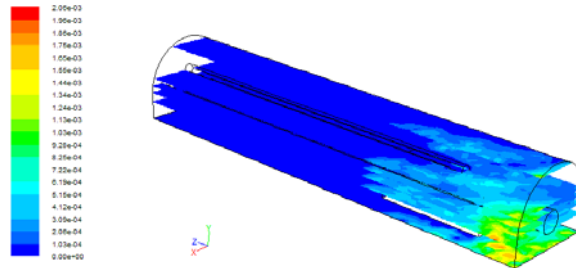
(c) 450m³/min
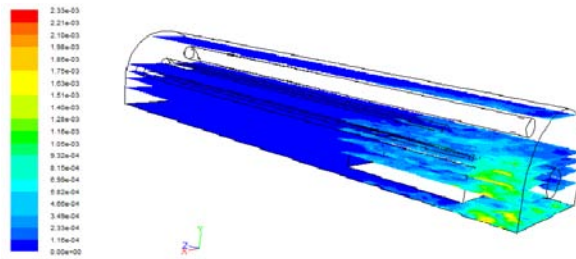
(d) 500m³/min
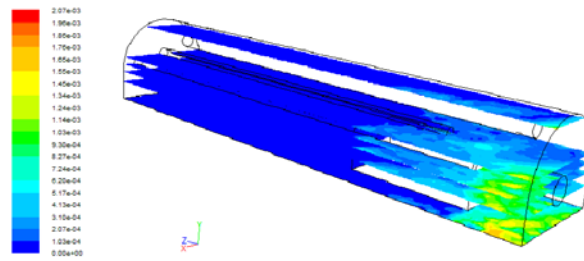
(e) 550m³/min
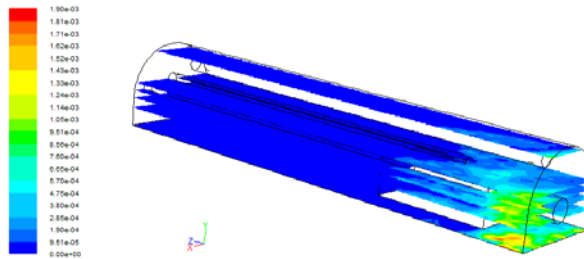
(f) 600m³/min

Fig. 4. The general trend of dust diffusion along the positive z-direction when different pumping air volume

Table 3. The different pumping air volume dust data of worker's breathing position in heading face

	320m³/min	400m³/min	450m³/min	500m³/min	550m³/min	600m³/min
C (m)	13.6	11.1	10.4	9.9	8.9	8.5
D ($mg/m^{3)}$)	368.4	270.2	238.5	227.1	201.6	179.5
E (mg/m^3)	338.9	264.5	219.6	202.1	181.2	147.4

According to figure 4 and table 3:

(1) With the increase of the amount of the pumping air, dust concentration of tunneling place decreases gradually from 2530mg/m³ to 1900mg/m³, which shows that the increase of the amount of the pumping air is beneficial to reduce the dust concentration around the tunneling place and prevent the aggregation of dust in tunneling place.

(2) Averaged dust concentration in driver's location and its whole section all steadily decrease, respectively from 368.4mg/m³, 338.9mg/m³ when the amount of the pumping air is 320m³/min to 179.5mg/m³, 147.4mg/m³ while it is 600m³/min, decreasing range up to 51.28% and 56.51%.

(3) With the increase of the amount of the pumping air, the diffusion distance of high concentration dust constantly decreases from tunneling place to other position, among then, the diffusion distance of high concentration dust reduces from 13.6m to 8.5m in other personnel cross section position (y=1.55), which means that increasing the pumping air can effectively inhibit the dust of tunneling place from spreading to roadway other region.

From the simulation results above, we can come to the following conclusions, when the amount of the pumping air is 600m³/min, the pumping dust ability of drawer-type wind tube is the strongest, which

can obviously inhibit the dust of tunneling place from spreading to roadway other region and which is the optimal pumping air of ventilating and dusting system.

6. The analysis of site application effect

According to above numerical simulation results indicate that: if we increase the amount of the pumping air of dusting fan up to 600m³/min in the heading face of Tangkou coal mine main return way, we will greatly decease the dust concentration of the face . So we change dusting fan of face to KCS-700 dust-clearing fan and collection efficiency will be about 95%, according to field measurement, pumping air of middle part and lateral part respectively being 309m³/min and 296m³/min, consistent with simulated conditions. Dust blower are replaced in the face of different locations before and after, the dust concentrations are measured on-site, selecting a total of three measuring points, 1# is the location of road header driver, 2# and 3# measuring points are chosen away from the side of the press-ventilated fan drum to 1m, height of 1.55m on the line, respectively, away from the tunneling place 10m and 20m.The simulation results and the measured values of different points' dust concentration are shown in table 4.

Table 4. Dust concentration of simulation value and fact value

Measuring Point Number	320m³/min		600m³/min	
	measured values (*mg/m³*)	simulated values (*mg/m³*)	measured values (*mg/m³*)	simulated values (*mg/m³*)
1#	392.1	368.4	163.4	179.5
2#	219.5	207.6	72.5	81.3
3#	128.4	90.8	51.6	42.2

The results can be seen from table 4: after the amount of pumping air increase to 600 m³/min in the south main return way's heading face, the dust concentration in three points decreases obviously, averaged dust-laying rate up to 61.7%, the dust concentration in driver's location decreasing from 392.1 m³/min to 163.4m³/min, the amplitude reduction up to 58.33%, significantly reducing dust concentration all over the face point. When the total amount of ventilation are 600m³/min 320 m³/min, in each measuring points, the simulation results are consistent with the measured values, which shows the simulation results can more accurately reflect dust diffusion laws with different ventilation in heading face.

7. Conclusions

Simulating numerically of dust diffusion laws with different amount of pumping air is simulated based on Fluent fluid simulation software, the results show that:
- When pushing air unchanged, the amount of ventilation in process of change from 320m³/min to 600m³/min, the pressure of the not drawing-type fan drum does not fluctuate largely. The pressure on the axis section of two different ports of drawing-type fan drum and the pressure of tunneling place and near the mouth of fan drum increase, indicating that increases the capacity of two fan drum.
- The increasing amount of ventilation reduces the dust accumulation in the tunneling place, suppresses dust spread to other areas of roadway, and significantly reduces the average dust concentration in the driver and the whole section.
- Among 6 amounts of the pumping air, when the amount of the pumping air is 600m³/min, the pumping dust ability of drawer-type wind tube is the strongest, which can obviously inhibit the dust

of tunneling place from spreading to roadway other region and which is the optimal pumping air of ventilating and dusting system.

- Field measurement indicates when the amount of pumping air is 600m^3/min and 320m^3/min, each face point value of the simulation results are consistent with the measured values, which shows that the simulation results more accurately reflect the dust diffusion laws with different pumping air in heading face.

Acknowledgments

References

[1] Zhao Yong-nian and Zhang Dou-jin. Application of mechanized rock roadway rapid drivage technology in jiulishan Mine[J]. *Zhongzhou Coal*, 2011, 181(01): 52-63. (in Chinese)

[2] Nie Wen, Cheng Wei-min and GuoYun-xiang. The research and application of air curtain closed-end dedusting system in full-heading face[J]. *Safety in Coal Mines*, 2009, 40(3): 19-22. (in Chinese)

[3] Li Qing, Yang Ren-Shu, Tang Zeng-lu, et al. Research on rapid excavation technology for deep mine large cross sectional rock roadway[J]. *Coal Science and Technology*, 2006, 34(10): 1-4. (in Chinese)

[4] Cheng Wei-min, Liu Xiang-sheng, Ruan guo-qiang, et al. The theory and technology of enclosure dust- laying model in speeded advance of coal road[J]. *Journal of China Coal Society,* 2009, 34(2): 203-207. (in Chinese)

[5] Klemens R., Kosinski P., Wolanski P., et al. Numerical study of dust lifting in a channel with vertical obstacles[J]. *Journal of Loss Prevention in the Process Industries*, 2001, 14(6): 469-473.

[6] Wang Hai-qiao. Study on jet ventilation flow field in heading face[J]. *Journal of China Coal Society*, 1999, 24(5): 498-501. (in Chinese)

[7] Wang Xiao-zhen, Jiang Zhong-an, Wang Shan, et al. Numerical simulation of distribution regularities of dust concentration during the ventilation process of coal roadway driving[J]. *Journal of China Coal Society*, 2007, 32(4): 386-390. (in Chinese)

[8] Nakayama, S. Uehino. K. and Inoue M.. 3 Dimensional flow measurement at heading face and application of CFD[J]. *Shigen·To·Sozai*, 1996, 112(9): 639-644.

[9] Zhang Jing, Wang Xiao-ling, Chen Hong-chao. et al. Simulation on ventilation and dust diffusion on heading face of the diversion tunnel[J]. *Journal of Hydroelectric Engineering*, 2008, 27(1): 111-117. (in Chinese)

[10] Zhou Li- xing and Gu H. X.. A non-linear k-ε-kp two-phase turbulence model[J]. *Journal of Fluids Engineering*, 2003, 125(1): 191-194. (in Chinese)

[11] Martin Sommerfeld. Validation of a stochastic lagrangian modeling approach for inters- particle collisions in homogeneous isotropic turbulence[J]. *International Journal of Multiphase Flow*, 2001, 27(10): 1829-1858.

[12] Zhou Li-xing and Xu Y.. Simulation of swirling gas-particle flows using an improved second-order moment two-phase turbulence model[J]. *Powder Technology*, 2001, 116(2-3): 178-189. (in Chinese)

[13] Soo S. L.. Particulate and Continuum Multiphase Fluid Dynamics[M]. London: Hemisphere Publishing Corporation, 1989.

[14] Yu Ming-gao, Guo Ming, Li Zhen-feng, et al. A numerical study of smoke development in a corridor[J]. *Journal of China University of Mining & Technology*, 2009, 38(1): 20-38. (in Chinese)

[15] Feng J., Hu H. H. and Joseph. D. D.. Direct simulation of initial value problems for the motion of solid bodies in a new tonian fluid [J]. *Journal of Fluid Mechanics*, 1994, 261: 95-134.

[16] Shao X. M., Liu Y. and Yu Z. S.. Interactions between two sedimenting particles with different sizes[J]. *Applied Mathematics and Mechanics: English Edition*, 2005, 26(3): 407-414.